ACS APPLIED MATERIALS & INTERFACES

Research Article

www.acsami.org

Encapsulation of an Adamantane-Doxorubicin Prodrug in pH-Responsive Polysaccharide Capsules for Controlled Release

Guo-Feng Luo, Xiao-Ding Xu, Jing Zhang, Juan Yang, Yu-Hui Gong, Qi Lei, Hui-Zhen Jia, Cao Li, Ren-Xi Zhuo, and Xian-Zheng Zhang*

Key Laboratory of Biomedical Polymers of Ministry of Education & Department of Chemistry, Wuhan University, Wuhan 430072, P.R. China

Supporting Information

ABSTRACT: Supramolecular microcapsules (SMCs) with the drug-loaded wall layers for pH-controlled drug delivery were designed and prepared. By using layer-by-layer (LbL) technique, the SMCs were constructed based on the self-assembly between polyaldenhyde dextran-graft-adamantane (PAD-*g*-AD) and carboxymethyl dextran-graft-*β*-CD (CMD-*g*-*β*-CD) on $CaCO_3$ particles via host-guest interaction. Simultaneously, adamantine-modified doxorubicin (AD-Dox) was also loaded on the LbL wall via host-guest interaction. The in vitro drug release study was carried out at different pHs. Because the AD groups were linked with PAD (PAD-*g*-AD) or Dox (AD-Dox) by pH-cleavable hydrazone bonds, AD moieties can be removed under the weak acidic condition, leading to destruction of SMCs and release of Dox. The pH-controlled drug release can enhance the uptake by tumor cells and thus achieve improved cancer therapy efficiency.

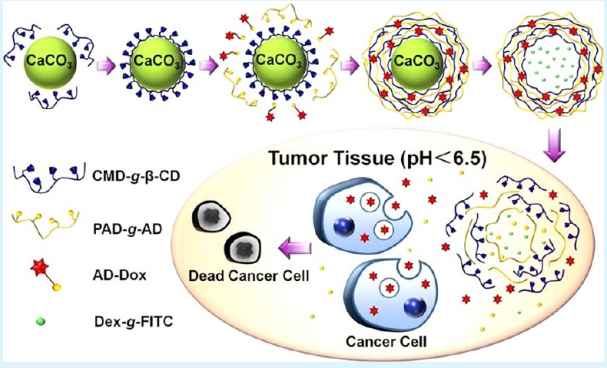

KEYWORDS: *self-assembly, supramolecular microcapsules, pH-responsive, drug controlled release*

1. INTRODUCTION

Because of the unfavorable side effects, the therapeutic effect of chemotherapy has been greatly limited for treatment of cancers.[1−3] Smart drug delivery system has been extensively studied to enhance the drug delivery efficiency with reduced side effects.[4,5] Recently, polymeric multilayer capsules (PMLCs) fabricated via layer-by-layer (LbL) technique with a controllable wall thickness, variable wall materials, and multifunctional properties have been interested investigated as drug carriers.[6−12] In particular, smart PMLCs responding to a range of stimuli, including redox-activation,[13] pH change,[14] magnetic field,[15] and light irradiation,[16] have been developed for various applications. In general, most of the hollow microcapsules are built on the basis of the electrostatic interaction among polyelectrolytes and drugs are usually loaded into their cores with high loading efficiency. However, the requirement of this loading method is that the drugs should have good water solubility and a relatively large molecular weight to avoid the leakage from the capsules.[17,18] Because many anti-tumor drugs, such as paclitaxel, curcumin, doxorubicin, and camptothecin, are small hydrophobic molecules, it is still a challenge to load and deliver these drugs by PMLCs.[2] Alternatively, researchers tried to load drugs on the layer wall of microcapsules.[19,20] However, the controllability of the drug release is not satisfied and the preparation process also seems a little bit complicated.

Compared with the traditional electrostatic-assembled hollow capsules, supramolecular microcapsules (SMCs) based on host−guest interaction between two types of molecules, typically cyclodextran (CD) and its guests,[21] have attracted much interest because the host−guest interaction is strong enough and generally not affected by pH value or ionic strength of the environment. For example, SMCs fabricated by alternately depositing of poly(allylamine hydrochloride)-graft-*β*-cyclodextrin and poly(allylamine hydrochloride)-graft-ferrocene show high stability and multi-responsiveness to the environmental stimuli and can serve as smart drug reservoir.[22] In our previous study, SMCs with photosensitivity were designed and investigated as a smart drug delivery system.[23]

The obvious change in pH from normal tissues (pH ∼7.4) to acidic cancerous tissues (pH <6.8)[24,25] has motivated researchers to design pH-sensitive drug delivery vehicles for tumor targeted delivery. In this work, a new kind of SMC with tumor-triggered drug release property was fabricated via host-guest interaction between polyaldenhyde dextran-graft-adamantane (PAD-*g*-AD) and carboxymethyl dextran-graft-*β*-CD (CMD-*g*-*β*-CD). The self-assembled microcapsules are pH-responsive because of the presence of acid-sensitive hydrazone bonds in PAD-*g*-AD. An anti-tumor drug, Dox[26,27] was

Received: July 7, 2012
Accepted: September 25, 2012
Published: September 25, 2012

conjugated with adamantine through hydrazone bonding and subsequently loaded on the wall of microcapsules via host–guest interaction. Under the weak acidic condition at tumor sites, AD groups in the structure of PAD-*g*-AD and AD-Dox could be removed because of the broken hydrazone bonds, leading to destruction of SMCs and release of Dox that can be subsequently uptaken in situ by tumor cells.

2. MATERIALS AND METHODS

2.1. Materials. Hydrazine hydrate, triethylamine (TEA), trifluoroacetic acid, *β*-cyclodextrin (*β*-CD), *p*-toluenesulfonic acid (*p*-TSA), *p*-toluenesulfonyl chloride (*p*-TsCl), ethylenediamine (EDA), ammonium choloride (NH_3·HCl), disodium ethylenediaminetetraacetate (EDTA), $NaBH_4$, potassium periodate (KIO_4), potassium carbonate (K_2CO_3), calcium chloride ($CaCl_2$), sodium hydroxide (NaOH), chloroacetic acid, isopropanol, dichloromethane, methanol, ethanol, hydrochloric acid, acetone, dimethylsulfoxide (DMSO), and *N*,*N*-dimethyl formamide (DMF) were purchased from Shanghai Reagent Chemical (P. R. China) and used as received. Dextran (M_w = 60–90 kDa) and poly(sodium 4-styrene-sulfonate) (PSS) (M_w = 70 kDa) were provided by Alfa Aesa China (Tianjin) and used as received. 1-Ethyl-3-(3-dimethyllaminopropyl)carbodiimide hydrochloride (EDC·HCl) and adamantine-1-carboxylic were obtained from Sigma-Aldrich and directly used. Doxorubicin hydrochloride (Dox·HCl) was purchased from Zhejiang Hisun Pharmaceutical Co. (China). Dulbecco's modified Eagle's medium (DMEM), fetal bovine serum (FBS) and Dulbecco's phosphatebuffered saline (PBS) were purchased from Invitrogen. All other reagents and solvents were of analytical grade and used directly. Dex-*g*-FITC (M_w = 20 kDa) and poly(aspartic-graft-adamantane) (PASP-*g*-AD) were synthesized according to our previous reports.[28,29]

2.2. Synthesis of Mono-6-deoxy-6-EDA-*β*-CD (EDA-*β*-CD). EDA-*β*-CD was synthesized according to our previous work.[30] To a solution of *β*-CD (10 g) in 240 mL of deionized (DI) water, was slowly added (1/3 mL/min) *p*-toluenesulfonyl chloride (2.6 g) to ensure that the substitution occurred at the C6 position. After vigorous agitation for 2 h at room temperature, 40 mL of NaOH (2.5 M) aqueous solution was added dropwise. Then, 12.0 g of ammonium chloride was added to the filtered suspension to adjust the solution pH to 8. The resultant solution was cooled to 4 °C and kept overnight. The crude product was collected by vacuum filtration followed by washing with acetone three times. Finally, the crude product was recrystallized at 60 °C to remove unreacted *p*-TsCl and *β*-CDs and then dried at 50 °C for 48 h under vacuum to obtain the final product of TsO-*β*-CD (4.92 g, yield: 30.6%).

EDA-*β*-CD was synthesized via the nucleophilic reaction between mono-6-(*p*-tolylsulfonyl)-*β*-cyclodextrin (TsO-*β*-CD) and ethylenediamine (EDA). Briefly, 5.0 g of TsO-*β*-CD was dissolved in 30 mL of anhydrous EDA and stirred at 80 °C for 48 h. Thereafter, the solution was cooled to room temperature and precipitated in acetone. The precipitation was washed with water/methanol (3:1, v/v) for three times to remove the residues. The product was dried at 50 °C for 48 h, resulting in a white powder of 1.63 g (yield: 33%).

2.3. Synthesis of Adamantine-1-carboxylic Acid Hydrazide (AD-NH-NH_2). AD-NH-NH_2 was synthesized according to the established procedure described elsewhere.[31] In brief, 0.55 g of adamantine-1-carboxylic was dissolved in 15 mL of dry methanol. Subsequently, 50 mg of *p*-toluenesulfonic acid (*p*-TSA) as dehydrating agent was added. After the mixture was refluxed at 85 °C for 24 h, the solvent was removed to give yellow oil. The crude product was dissolved in 5 mL of dichloromethane and washed with DI water for three times. The organic phase was collected and dried over $MgSO_4$, filtered, evaporated, and finally dried under vacuum for 24 h to obtain 0.54 g of methyl adamantine-1-carboxylate (yield: 92%).

Subsequently, 0.2 g of the synthesized methyl-adamantane-1-carboxylate was dissolved in 4 mL of ethanol and then 20 mL of hydrazine hydrate as well as 50 μL of triethylamine as a catalyst was added. After refluxing at 85 °C for 24 h, the solvent was removed. The crude product was purified by dissolving in 5 mL of dichloromethane and then washing with DI water three times. The organic phases were collected and dried over $MgSO_4$, filtered, and finally evaporated to obtain 0.19 g of adamantine-1-carboxylic acid hydrazide (yield: 96%).

2.4. Synthesis of Adamantine-Modified Doxorubicin (AD-Dox). Sixty-seven milligrams of adamantine-1-carboxylic acid hydrazide and 100 mg of doxorubicin hydrochloride were dissolved in 50 mL of dry methanol. Thereafter, 50 μL of trifluoroacetic acid was added as a catalyst. The mixture was refluxed at 50 °C for 48 h in dark. The solution was then concentrated by rotary evaporation and precipitated in ethyl acetate for three times. The product was collected by centrifugation and dried under vacuum to obtain 80 mg of AD-Dox (yield: 32%).

2.5. Synthesis of Polyaldenhyde Dextran-graft-adamantane (PAD-*g*-AD). Dextran was oxidized by periodate oxidation. 0.3 g of PAD was dissolved in 15 mL of distilled water and 0.123 g of AD-NH-NH_2 (35% of PAD repeat unit) in 15 mL of DMSO was added dropwise with vigorous stirring. The mixture was stirred at 30 °C for 24 h, followed by dialyzing (MWCO 8-12 kDa) against DMSO for 2 days and then DI water for 3 days. The resulting dialysis solution was finally lyophilized to give 0.21 g of PAD-*g*-AD (yield: 24.4%).

2.6. Synthesis of Carboxymethyl Dextran-graft-*β*-CD (CMD-*g*-*β*-CD). Dextran was first reacted with chloroacetic acid to obtain carboxymethyl dextran (CMD) according to published procedure.[32] Then, EDA-*β*-CD was grafted to CMD using EDC as the coupling reagent. Briefly, 0.667 g of CMD and 3.15 g of EDA-*β*-CD (65% of CMD repeat unit) were dissolved in 50 mL of distilled water, and the pH of the solution was then adjusted to 5.0 by using 1 M HCl solution. After being stirred at room temperature for 30 min, 0.783 g of EDC (n_{COOH}/n_{EDC} = 1/1.2) was dissolved in 10 mL of distilled water and slowly added. After the reaction at room temperature for 24 h, the solution was dialyzed (MWCO 8-12 kDa) against distilled water for 3 days and finally lyophilized to give 0.42 g of CMD-*g*-*β*-CD (yield: 43%).

2.7. Preparation of Dex-*g*-FITC Captured by $CaCO_3$ Particles. Seven and a half milliliters of K_2CO_3 aqueous solution (0.33 M) containing 15 mg of Dex-*g*-FITC was rapidly poured into 7.5 mL of $CaCl_2$ aqueous solution (0.33 M) containing 15 mg of PSS. After intense agitation for 30 s, the reaction mixture was allowed to stir for 2 min. Thereafter, the precipitate was filtered off, followed by washing with DI water and acetone and drying in air.[33] Note that Dex-*g*-FITC was used as a model drug to label the inner core with green fluorescence.

2.8. Synthesis of (CMD-*g*-*β*-CD/(PAD-*g*-AD&AD-Dox))$_4$ and Preparation of (CMD-*g*-*β*-CD/(PAD-*g*-AD&Dox))$_4$ Microcapsules. Dex-*g*-FITC-captured $CaCO_3$ particles were used as colloid template for the fabrication of microcapsules. To absorb the CMD-*g*-*β*-CD and PAD-*g*-AD on the surface, $CaCO_3$ particles were coated with PAH and PASP-*g*-AD prior via electrostatic interaction. Approximately 100 mg of $CaCO_3$ particles and 1 mL of PAH aqueous solution (1 mg/mL) were mixed and the mixture was shaken for 15 min to establish a PAH layer. After adsorption, the particles were isolated by centrifugation (10,000 rpm for 1 min), followed by washing with DI water three times. For adsorption of the next layer, 1 mL of PASP-*g*-AD aqueous solution (1 mg/mL) was added, followed by the same washing protocol. After that, the LbL assembly between CMD-*g*-*β*-CD and PAD-*g*-AD & AD-Dox (containing 1 mg/mL PAD-*g*-AD and 20 nmol/mL AD-Dox) (or PAD-*g*-AD&Dox (containing 1 mg/mL PAD-*g*-AD and 20 nmol/mL Dox)) on $CaCO_3$ particles was performed by the same method. The LbL process was repeated to get the microcapsules with a designed number of layers. The whole process was protected from light wherever possible.

To reduce the hydrazine bonds in the microcapsules, 100 mg of $CaCO_3$ particles coated with four bilayers of CMD-*g*-*β*-CD/(PAD-*g*-AD&AD-Dox) films were dispersed in 2 mL of $NaBH_4$ aqueous solution (4 mg/mL) and then shaken for 6 h. After reduction, the particles were isolated by centrifugation (10 000 rpm for 1 min), followed by washing with DI water three times.

Hollow microcapsules were collected by dissolving the $CaCO_3$ core using EDTA aqueous solution (pH 7.4, 0.4 M). The microcapsules

Scheme 1. Synthesis Routes of AD-Dox (4), CMD-*g*-*β*-CD (5) and PAD-*g*-AD (6)

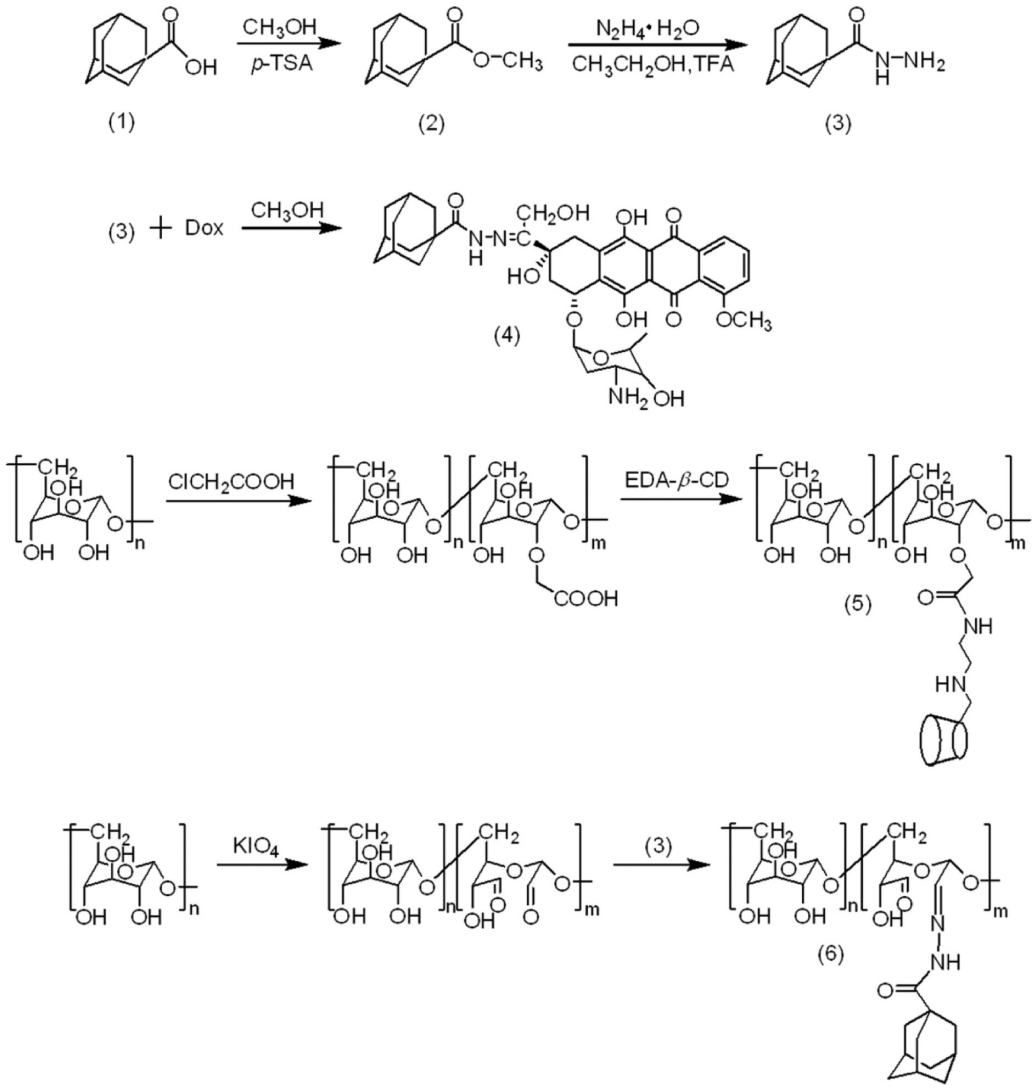

were isolated by centrifugation (10 000 rpm for 1 min) and washed with DI water three times to remove the residual EDTA.

2.9. Characterization. ^{1}H NMR spectra were recorded on a Mercury VX-300 spectrometer at 300 MHz (Varian, U.S.) by using TMS as an internal standard. The molecular weights and the molecular weight distributions of CMD and CMD-*g*-*β*-CD were determined by a size exclusion chromatography and multi-angle laser light scattering (SEC-MALLS) system consisting of a MALLS device (DAWN EOS, Wyatt Technology) and an interferometric refractometer (a differential refractive index detector) (Optilab DSP, Wyatt Technology). The data were analyzed with Astra software (Wyatt Technology). The molecular weight of AD-Dox was analyzed by electrospray ionization mass spectrometry (ESI-MS, LCQ Advantage, Finigan, USA). Fourier transform infrared spectroscopy (FT-IR) spectra were collected on a Perkin-Elmer spectrophotometer by pressing the sample into potassium bromide (KBr) pellet.

The morphology of the hollow capsules was viewed by using confocal laser scanning microscopy (CLSM, C1-si, Nikon, Japan) and scanning electron microscopy (SEM, FEI-QUANTA 200). For SEM observation, a drop of the capsule solution was deposited onto a glass slide. After drying, the sample was fixed on an aluminum stub and coated with gold for 80 s.

2.10. Acid Destruction of (CMD-*g*-*β*-CD/(PAD-*g*-AD&AD-Dox))$_4$ Microcapsules. To investigate the acid destruction behavior of (CMD-*g*-*β*-CD/(PAD-*g*-AD&AD-Dox))$_4$ microcapsules, a fixed amount of the hollow capsules was incubated in 1 mL of buffer solution (0.1 M) at a pH of 5.5 or 7.4 for 6 h, followed by observation under CLSM continuously.

2.11. In vitro Drug Release at Different pH Values. 100 mg of $CaCO_3$ particles coated with four bilayers of CMD-*g*-*β*-CD/(PAD-*g*-AD&AD-Dox) films were incubated in 1 mL of EDTA (pH 7.4, 0.4 M) aqueous solution to remove the core. Then, the microcapsules were isolated with centrifugation (10,000 rpm for 1 min) and dispersed in 1 mL of distilled water. The CMD-*g*-*β*-CD/(PAD-*g*-AD&AD-Dox) capsule solution was evenly divided into two parts and respectively put into two dialysis tubes (MWCO 8-12 kDa). The dialysis tube was then immersed into 10 mL of buffer solution (0.1 M) at a pH of 7.4 or 5.5. Samples were withdrawn from the solution periodically and fresh 10 mL of medium was added. The amount of Dox released from the capsules was measured on an RF-530/PC spectrofluorophotometer (Shimadzu) with absorbance at 557 nm (excitation wavelength used was 484 nm). The cumulative drug release was calculated as follows: cumulative amount release (%) = $(M_t/M_0) \times 100$, where M_t is the amount of drug released from the capsules at time t and M_0 is the amount of drug loaded in the capsules. To determine the amount of drug loaded in the microcapsules, we freeze-dried a fixed amount of the drug-loaded capsule solution. The lyophilized microcapsules were then dissolved in 0.1 M HCl to destroy the structure and then the Dox concentration was measured the fluorescence emission at 557 nm.

The drug release behaviors of (CMD-*g*-*β*-CD/(PAD-*g*-AD&AD-Dox))$_4$ microcapsules reduced with $NaBH_4$ at pH 5.5, (CMD-*g*-*β*-

CD/(PAD-*g*-AD&Dox))$_4$ microcapsules at pH 5.5 and 7.4 were also examined by using the same method described above.

2.12. Co-incubation of (CMD-*g*-*β*-CD/(PAD-*g*-AD&AD-Dox))$_4$ Microcapsules with HeLa Cells at Different pHs. Human cervix carcinoma (HeLa) cells were incubated in DMEM medium with 10% FBS and 1% antibiotics (penicillin−streptomycin, 10 000 U/mL) (37 °C, 5% CO_2). The cells were seeded, respectively, into a six-well plate (1×10^5 cells/well) and then incubated in 1 mL of DMEM containing 10% FBS for 24 h. Subsequently, the culture medium was removed and replaced with DMEM containing AD-Dox loaded microcapsules (70 μg, containing ~0.6 μg Dox) at a pH of 7.4 or 5.5. After incubating for 4 h and then removing the medium, the cells were washed with PBS buffer (pH 7.4) for three times and finally viewed under CLSM.

2.13. In vitro Cytotoxicity Assay. MTT assay was employed to evaluate the cytotoxicity of microcapsules to HeLa cells. In brief, HeLa cells were seeded in 96-well plates (6000 cells/well, containing 100 μL DMEM) and incubated for 1 day. Thereafter, the microcapsules, AD-Dox loaded microcapsules or free AD-Dox dispersed in DMEM at a pH of 7.4 or 5.5 were added, respectively. After incubating the cells at 37 °C for 24 h, the medium was replaced with 200 μL of fresh medium and 20 μL of MTT (5 mg/mL) solution was added to each well. After incubation for another 4 h, the medium was removed and 150 μL of DMSO was added to each well. The absorbance was measured at 570 nm using a microplate reader (Bio-Rad, Model 550, USA). The relative cell viability was calculated as follows: cell viability (%) = ($OD_{570\ (sample)}/OD_{570\ (comtrol)}$) × 100, where $OD_{570\ (control)}$ is obtained in the absence of microcapsules, whereas $OD_{570\ (sample)}$ is obtained in the presence of microcapsules. Each value was averaged from four independent experiments.

3. RESULTS AND DISCUSSION

3.1. Synthesis of AD-Dox, PAD-*g*-AD, and CMD-*g*-*β*-CD. As shown in Scheme 1, adamantine-1-carboxylic (**1**) was first carboxylated to obtain the methyl adamantine-1-carboxylate (**2**), which was used to react with hydrazine to prepare AD-NH-NH_2 (**3**). AD-Dox (**4**) was synthesized from AD-NH-NH_2 and Dox to form the well-known acid-cleavable hydrazone bond between C-13 carbonyl of Dox and hydrazides.[34,35] From the ^{1}H NMR spectra revealed in Figure 1, the signal located at δ 3.65 ppm was assigned to the protons of the methyl in AD-COO−CH_3 (Figure 1a). After the reaction with hydrazide (Figure 1b), this signal disappeared and two new signals located at δ 5.30 and 6.96 ppm corresponding to the protons of -NH- and -NH_2 of AD-CO-NH-NH_2, respectively, could be observed. The ^{1}H NMR spectrum of AD-Dox is presented in Figure 1c.

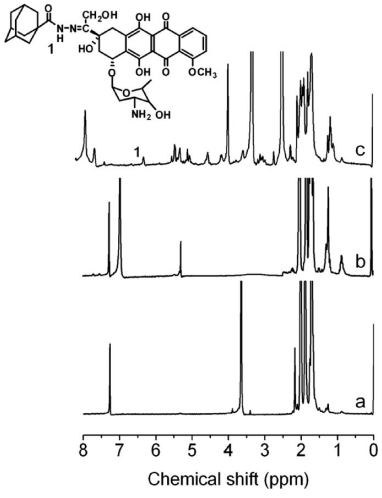

Figure 1. ^{1}H NMR spectra of (a) AD-COO-CH_3, (b) AD-CO-NH-NH_2, and (c) AD-NH-N=C-Dox.

The signal located at δ 6.35 ppm belonged to the protons of -NH- of hydrazide and the signals located at δ 1.5−2.0 ppm became significantly enhanced, which was attributed to the protons of AD. Moreover, the molecular weight of AD-Dox found in electrospray ionization mass spectrometry (ESI-MS) ($C_{38}H_{35}N_3O_{11}^+$) was 720.2 g/mol, which was consistent with calculated 720.31 g/mol, demonstrating the success in the synthesis of AD-Dox.

PAD-*g*-AD with an acid-cleavable hydrazone bond was synthesized from PAD and AD-NH-NH_2. The successful synthesis of PAD-*g*-AD was proved by ^{1}H NMR spectrum revealed in Figure 2, and the substitution degree of AD in PAD-

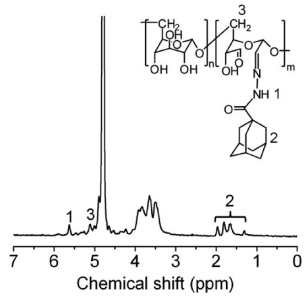

Figure 2. ^{1}H NMR spectrum of PAD-*g*-AD.

g-AD was calculated to be ~21%. The structure of PAD-*g*-AD was also confirmed by FT-IR spectrum displayed in Figure 3a.

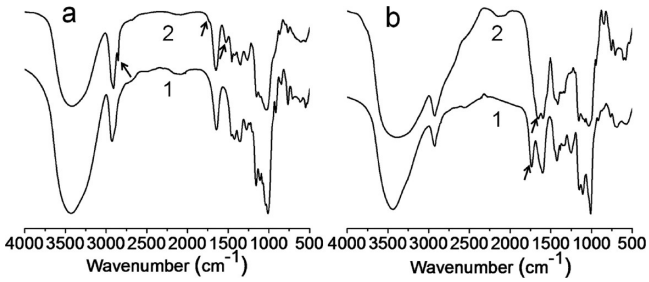

Figure 3. FT-IR spectra of (a) PAD (1) and PAD-*g*-AD (2), (b) CMD (1) and CMD-*g*-*β*-CD (2).

Compared with the FT-IR spectrum of PAD, the weak band at 1662 cm^{-1} was attributed to the C=N stretching, which appeared as a shoulder because of the overlap of N−H stretching band at 1600 cm^{-1}. The bands at 1525 (N−H bending) and 2852 cm^{-1} (C−H stretching in hydrazone bond) also demonstrated the formation of hydrazone bonds.[35,36]

CMD-*g*-*β*-CD was synthesized from CMD and EDC-*β*-CD by using EDC as a coupling reagent. The number of carboxyl groups to the anhydroglucose unit of CMD was calculated as 83% based on the corresponding ^{1}H NMR spectrum. Because the compounds of CMD and *β*-CD have the similar repeat units, it is difficult to compare their structures by ^{1}H NMR. FT-IR was employed to examine the structure of CMD-*g*-*β*-CD. As shown in Figure 3b, the characteristic band at 1730 cm^{-1} was ascribed to carboxyl group in CMD. After the reaction with *β*-CD, the band at 1730 cm^{-1} disappeared and a new band at 1650 cm^{-1} (amide group of CMD-*g*-*β*-CD) could be observed, indicating the complete conversion from the carboxyl groups of CMD to the amide groups of CMD-*g*-*β*-CD.[23]

As measured by SEC-MALLS, the weight-average molecular weights (M_w) of CMD and CMD-*g*-*β*-CD were 111 200 g/mol

Scheme 2. Schematic Diagram of the pH-Induced Drug Release from a Drug Loaded Microcapsule

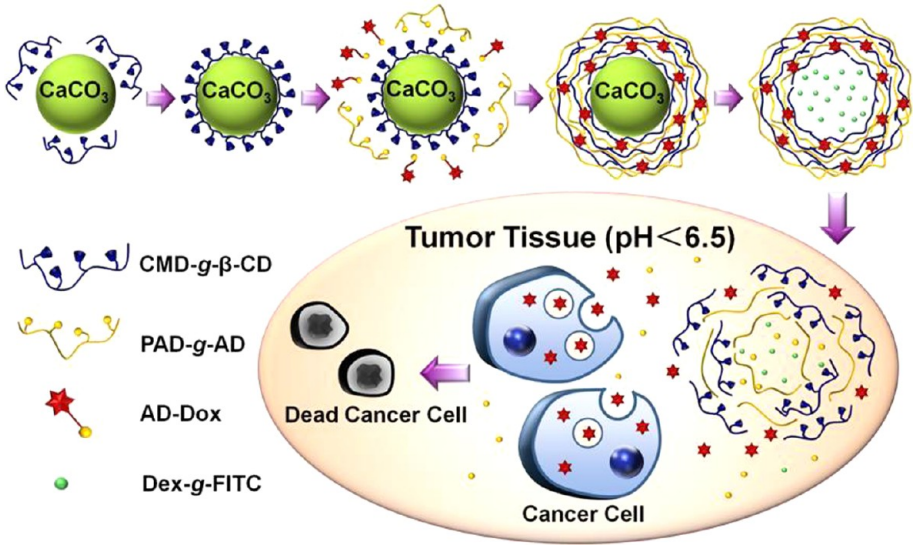

(M_w/M_n = 1.57) and 489 300 g/mol (M_w/M_n = 2.00), respectively, and the substitution degree (SD) of β-CD in CMD-*g*-β-CD was thus calculated as 50%.

3.2. Fabrication of (CMD-*g*-β-CD/(PAD-*g*-AD&AD-Dox))$_4$ or (CMD-*g*-β-CD/(PAD-*g*-AD&Dox))$_4$ Microcapsules. The LbL assembly on $CaCO_3$ particles captured with Dex-*g*-FITC was performed by alternately depositing of CMD-*g*-β-CD and PAD-*g*-AD&AD-Dox. Hollow microcapsules were obtained by dissolving the core in EDTA solution as shown in Scheme 2. The confocal laser scanning microscopy (CLSM) and scanning electron microscopy (SEM) images of the (CMD-*g*-β-CD/(PAD-*g*-AD&AD-Dox))$_4$ microcapsules are shown in Figure 4. As shown in Figure 4a, the red fluorescence from Dox with an excitatation wavelength of 543 nm could be observed in the coronas of microcapsules. In Figure 4b, the inner core was excitated by a laser with a wavelength 488 nm to give bright green fluorescence, implying the presence of Dex-*g*-FITC in the cores of the microcapsules. Figure 4c displays the fluorescent image of the microcapsules loaded with AD-Dox on the wall layers and Dex-*g*-FITC in the cores. Also, weak red fluorescence could be observed in the internal core because of the diffusion of a small part of AD-Dox into the $CaCO_3$ core during the LbL assembly process. SEM images presented in Figure 4d indicated that the microcapsules were intact even though they collapsed after air-drying. All these results strongly demonstrated that regular spherical microcapsules remained intact after core removal and could disperse separately in water.

In this study, we have also prepared (CMD-*g*-β-CD/(PAD-*g*-AD&Dox))$_4$ microcapsules and their CLSM images are shown in Figure 5. When excited by laser at 543 nm (Figure 5a), because of the presence of physically absorbed Dox on the wall layers, all the microcapsules presented regular red coronas. Being similar to the microcapsules of (CMD-*g*-β-CD/(PAD-*g*-AD&AD-Dox))$_4$, Dex-*g*-FITC could be also captured in the core and presented green fluorescence. The CLSM image in Figure 5c revealed that regular microcapsules with intact core-shell structure and diameter of ~4 μm could disperse separately in distilled water.

3.3. Acid Destruction of (CMD-*g*-β-CD/(PAD-*g*-AD&AD-Dox))$_4$ Microcapsules. As we know, the pH around cancerous tissues is more acidic (pH < 6).[28,37,38] The hydrazine

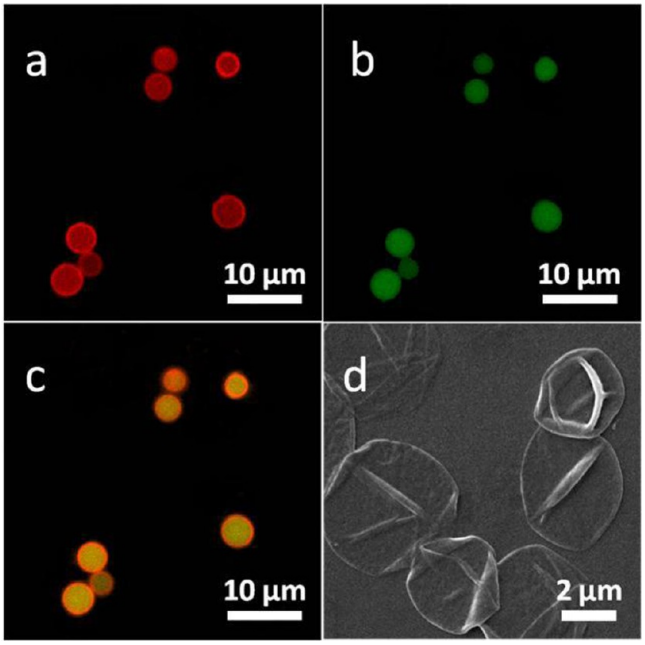

Figure 4. (a–c) CLSM images of (CMD-*g*-β-CD/(PAD-*g*-AD&AD-Dox))$_4$ microcapsules (a: red fluorescence image, b: green fluorescence image, and c: overlapped images of red and green fluorescences). (d) SEM image of (CMD-*g*-β-CD/(PAD-*g*-AD&AD-Dox))$_4$ microcapsules.

bonds incorporated to the microcapsules could be cleaved under this condition.[36] To prove the destruction of (CMD-*g*-β-CD/(PAD-*g*-AD&AD-Dox))$_4$ microcapsules under weak acidic condition, the microcapsules were incubated in the buffer solution at pH 5.5 or 7.4. As shown in Figure 6, after removing the core by immersing the microcapsules in acetate buffer solution (pH 5.5, 0.1 M), the microcapsules still maintained the integrity of the core-shell structure (Figure 6a). The red fluorescent AD-Dox (Figure 6a$_1$) and green fluorescent Dex-*g*-FITC (Figure 6a$_2$) were still loaded completely in the intact shells and cores of (CMD-*g*-β-CD/(PAD-*g*-AD&AD-Dox))$_4$ microcapsules. Moreover, both red and green fluorescent intensities are strong at the initial stage of destruction. The

dx.doi.org/10.1021/am301258a | ACS Appl. Mater. Interfaces 2012, 4, 5317–5324

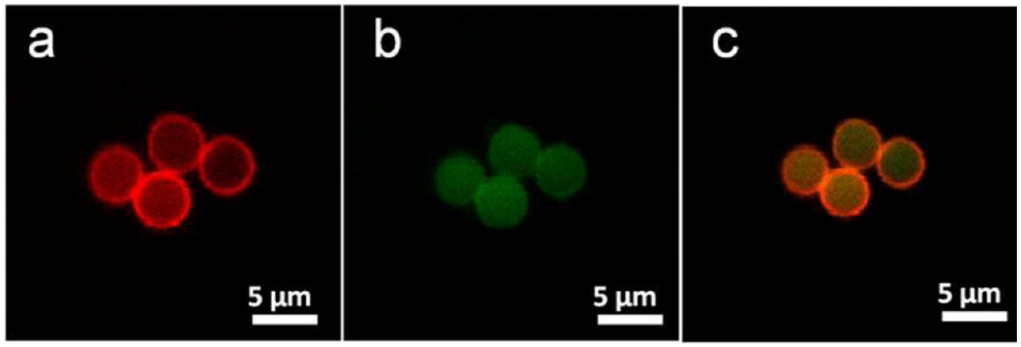

Figure 5. CLSM images of $(CMD\text{-}g\text{-}\beta\text{-}CD/(PAD\text{-}g\text{-}AD\&Dox))_4$ microcapsules: (a) red fluorescent Dox loaded on the wall, (b) green fluorescent Dex-*g*-FITC captured in the core, (c) overlay of part a and b.

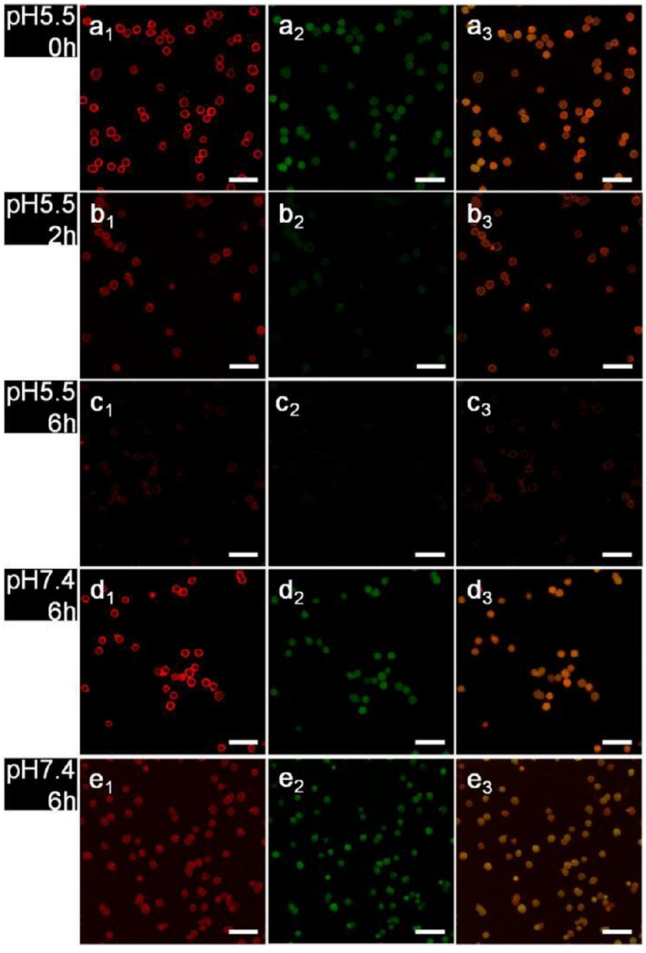

Figure 6. CLSM images of destruction of (a–d) $(CMD\text{-}g\text{-}\beta\text{-}CD/(PAD\text{-}g\text{-}AD\&AD\text{-}Dox))_4$ microcapsules at different pHs, (e) $(CMD\text{-}g\text{-}\beta\text{-}CD/(PAD\text{-}g\text{-}AD\&Dox))_4$ microcapsules incubated in pH 7.4 buffer solution for 6 h. (a_1, b_1, c_1, d_1, e_1) Red fluorescent Dox, (a_2, b_2, c_2, d_2, e_2) green fluorescent Dex-*g*-FITC, and (a_3, b_3, c_3, d_3, e_3) overlays of (a_1, a_2), (b_1, b_2), (c_1, c_2), (d_1, d_2), and (e_1, e_2), respectively. The scale bar is 10 μm.

CLSM images of the capsules after immersed in the solution at pH 5.5 for 2 and 6 h are shown in images b and c in Figure 6, respectively. The intensity of red fluorescence of AD-Dox on the shells (Figure $6b_1$, c_1) and green fluorescence of Dex-*g*-FITC encapsulated in the cores (Figure $6b_2$, c_2) decreased significantly 2 h later. Because of the hydrolysis of the hydrazone bond between AD moiety and PAD chain, the core-shell structure was destructed after being immersed in the buffer solution with pH 5.5 for 6 h (Figure 6c). In contrast, the red fluorescent shells (Figure $6d_1$) and green fluorescent cores (Figure $6d_2$) of the microcapsules did not show obvious changes after being immersed in the solution with pH 7.4 for 6 h, implying that the drug loaded microcapsules could maintain long-term stability under physiological pH. All these results indicated that $(CMD\text{-}g\text{-}\beta\text{-}CD/(PAD\text{-}g\text{-}AD\&AD\text{-}Dox))_4$ microcapsules could be disrupted under weak acidic condition while maintaining the core-shell structure under physiological pH.

To confirm that AD-Dox on the wall layers was loaded through host-guest interaction with CMD-*g*-β-CD rather than physical adsorption, $(CMD\text{-}g\text{-}\beta\text{-}CD/(PAD\text{-}g\text{-}AD\&Dox))_4$ microcapsules were prepared for comparison. The CLSM images of the microcapsules loaded with Dox were similar to the microcapsules loaded with AD-Dox as shown in Figure 5. After being incubated in PBS buffer solution (0.1 M, pH 7.4) for 6 h, CLSM images of the microcapsules were taken and shown Figure 6e. In comparison with the images presented in Figure 6d, the green fluorescent Dex-*g*-FITC (Figure $6e_2$) was still encapsulated in the core, whereas the red fluorescence of free Dox (Figure $6e_1$) in the background increased obviously, implying that Dox diffused out from $(CMD\text{-}g\text{-}\beta\text{-}CD/(PAD\text{-}g\text{-}AD\&Dox))_4$ microcapsules because of the absence of host–guest interaction.

3.4. In vitro Drug Release at Different pHs. The drug release behaviors of $(CMD\text{-}g\text{-}\beta\text{-}CD/(PAD\text{-}g\text{-}AD\&AD\text{-}Dox))_4$ microcapsules were studied at pH of 7.4 and 5.5, respectively. The loading content of Dox in the microcapsules was calculated as 0.86 wt.%. As shown in Figure 7a, at pH 7.4, the drug was released slowly and only 18% of the loaded drug was released within 13 h. The main reason was attributed to the physical adsorption of a small amount of AD-Dox. However, at an acidic

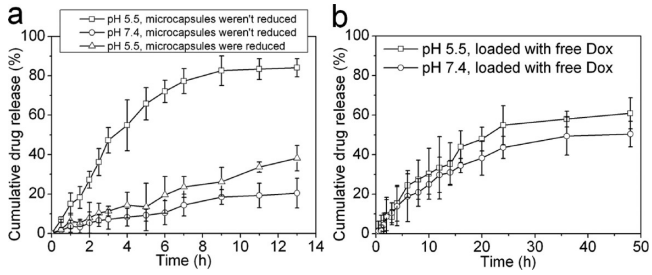

Figure 7. Drug release profiles of (a) non-reduced microcapsules at pH 7.4 and 5.5 and reduced microcapsules at pH 5.5; (b) microcapsules loaded with Dox at pH 7.4 and 5.5.

pH of 5.5, a dramatically increased drug release was observed and about 80% of loaded drug was released within 13 h. For comparison, the drug release property of the reduced microcapsules was studied at pH 5.5. The disappearance of band at 1647 cm^{-1}, which was attributed to the C═N stretching in FT-IR spectrum (see Figure S1 in the Supporting Information) confirmed the successful reduction of microcapsules. As shown in Figure 7a, around 37% of the loaded drug was released within 13 h, which was much lower than the non-reduced microcapsules at pH 5.5. This difference was attributed to the hydrolysis of hydrazone bond between AD moiety and Dox. Because of the fact that the pH value may have some influence on the interaction between AD and CD,[39,40] the amount of drug released from reduced microcapsules at pH 5.5 was slightly higher than the non-reduced ones at pH 7.4. Moreover, the drug release behavior of microcapsules loaded with Dox was also studied. As shown in Figure 7b, no obvious change in drug release could be observed at different pHs. All the results strongly demonstrated that the drug loaded on the wall layers of microcapsules can be efficiently inhibited at a pH of 7.4, whereas they are released rapidly in response to a weak acidic environment.

3.5. Co-incubation of (CMD-*g*-*β*-CD/(PAD-*g*-AD&AD-Dox))$_4$ Microcapsules with HeLa cells at Different pHs. To examine the pH dependent drug release behavior of microcapsules and cell uptake of the drug, (CMD-*g*-*β*-CD/(PAD-*g*-AD&AD-Dox))$_4$ microcapsules were incubated with HeLa cells for 4 h at different pHs. In this work, after co-incubation, the medium was removed and cells were washed with fresh PBS prior to observing under CLSM. As shown in Figure 8, at pH 7.4, the faint red fluorescence in HeLa cells

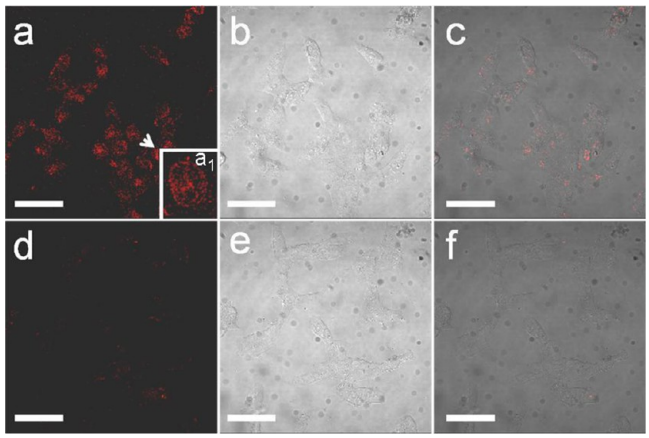

Figure 8. CLSM images of HeLa cells treated with AD-Dox loaded microcapsules at (a–c) pH 5.5 and (d–f) pH 7.4. (a_1) Enlarged image as the arrow indicated. (a, d) Dox fluorescence in cells, (b, e) phase contrast images, (c, f) overlay of fluorescence images and phase contrast images. The scale bar is 50 μm.

indicated that only a small amount of Dox was released and uptaken by tumor cells because hydrazone bonds did not cleave at this pH, implying that the drug loaded microcapsules were stable under human physiological conditions. However, at a pH of 5.5, about 50% of loaded Dox could be released within 4 h (Figure 7a), the red fluorescence with a relatively high intensity could be observed (Figure 8a) because of the in situ uptake of Dox by HeLa cells. And the image with higher magnification (Figure 8a_1) showed that only Dox was found in HeLa cells. Obviously, the drug release behavior of drug loaded SMCs can be controlled by pHs.

3.6. In vitro Cytotoxicity of (CMD-*g*-*β*-CD/(PAD-*g*-AD&AD-Dox))$_4$ Microcapsules. To evaluate the effect of pH alone on the viability of HeLa cells, we carried out correlative experiment and results were shown in Figure S2 in the Supporting Information. After 48 h incubation, the cell proliferation was reduced by 24% from a pH of 7.4 to 5.5, indicating that the low pH value was unfavorable on cell growth. As shown in Figure 9a, after incubation with the

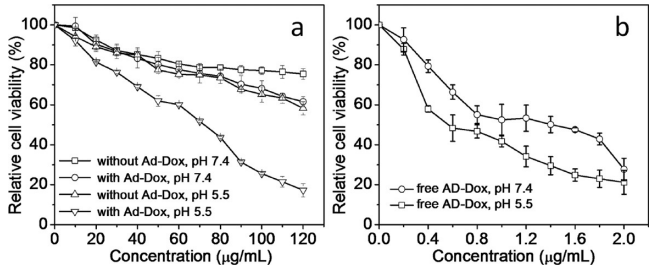

Figure 9. Viability of HeLa cells incubated with (a) the microcapsules with or without AD-Dox at different pHs for 48 h and (b) free AD-Dox at different pHs for 48 h.

microcapsules without AD-Dox at a pH of 5.5 or 7.4 for 48 h, the cell viability was above 60% when the microcapsule concentration was below 120 μg/mL, indicating that the microcapsules have a low cytotoxicity at both pH 7.4 and 5.5. After incubation with AD-Dox loaded microcapsules for 48 h at pH 7.4, the cell viability was around 70% and slightly decreased with the increasing concentration of AD-Dox loaded microcapsules. As expected, when the pH was adjusted to 5.5, the cell viability decreased dramatically and the viability deceased with the increasing concentration of drug loaded microcapsules, due to the fact that the drugs could be triggered release under weak acidic condition. This pH-dependent cell growth inhibition effect is desirable to achieve improved therapy efficiency for tumor treatment since cancerous tissues have a lower pH (pH <6.8) compared to normal tissues (pH ~7.4). The cell viability of HeLa cells incubated with free AD-Dox was also studied and the result is presented in Figure 9b. Obviously, the cell viability treated by AD-Dox at pH 5.5 reduced by ~20% compared with that at pH 7.4. According to the data of Figure 7, more than 80 % of the loaded Dox was released within 13 h at pH 5.5. Therefore, the concentration of Dox released from the microcapsules was ~0.70 μg/mL within 13 h when the concentration of drug loaded microcapsules was 100 μg/mL. On the basis of the cytotoxicity of free Dox in HeLa cells in our previous work,[29] at this concentration, the cell viability was 27%. The result of this study was consistent with the literature report. Compared with the cytotoxicity of free AD-Dox at the concentration of 0.7 μg/mL, the cell viability remained above 50% as presented in Figure 9b, suggesting that the cytotoxicity of microcapsules was attributed to the released cytotoxic Dox rather than AD-Dox.

4. CONCLUSIONS

In summary, a new class of smart SMCs was designed and fabricated for pH-controlled drug delivery. AD-Dox, a pH-sensitive prodrug, can be effectively loaded on the microcapsule walls. Drug release study confirmed that the SMCs could be destructed under weak acidic environment, leading to rapid

drug release from SMCs due to the breakage of the pH-cleavable hydrazone bonds. In vitro studies showed that the cytotoxicity of these drug-loaded SMCs under physiological condition was much lower than that at acidic condition. Upon the trigger of acidic environment, the loaded drug can be released rapidly to induce tumor cell apoptosis. These SCMs with tumor triggered release behavior will find great potential in tumor chemotherapy.

■ ASSOCIATED CONTENT

Supporting Information

Additional figures (PDF). This material is available free of charge via the Internet at http://pubs.acs.org.

■ AUTHOR INFORMATION

Corresponding Author

*Tel.: + 86 27 6875 5993. Fax: + 86 27 6875 4509. E-mail: xz-zhang@whu.edu.cn (X.Z.Z.).

Notes

The authors declare no competing financial interest.

■ ACKNOWLEDGMENTS

This work was financially supported by the Ministry of Science and Technology of China (2011CB606202), National Natural Science Funds for Distinguished Young scholar (51125014), the Research Fund for the Doctoral Program of Education of China, and the Planning Project of Innovative Experiment of National Undergraduate (091048617).

■ REFERENCES

(1) Bisht, S.; Maitra, A. *Nanomed. Nanobiotechnol.* **2009**, *1*, 415−425.
(2) Chilkoti, A.; Dreher, M. R.; Meyer, D. E.; Raucher, D. *Adv. Drug Delivery. Rev.* **2001**, *54*, 613−630.
(3) Chari, R. V. J. *Adv. Drug Delivery. Rev.* **1998**, *31*, 89−104.
(4) Allen, T. M.; Cullis, P. R. *Science* **2004**, *303*, 1818−1822.
(5) Wang, C.; Li, Z.; Cao, D.; Zhao, Y. L.; Gaines, J. W.; Bozdemir, O. A.; Ambrogio, M. W.; Frasconi, M.; Botros, Y. Y.; Zink, J. I.; Stoddart, J. F. *Angew. Chem., Int. Ed.* **2012**, *51*, 1−7.
(6) Yan, Y.; Wang, Y.; Heath, J. K.; Nice, E. C.; Caruso, F. *Adv. Mater.* **2011**, *23*, 3916−1921.
(7) Liang, K.; Such, G. K.; Zhu, Z.; Yan, Y.; Lomas, H.; Caruso, F. *Adv. Mater.* **2011**, *23*, 273−277.
(8) De Koker, S.; Vervaet, C.; Remon, J. P.; De Geest, B. G. *J. Controlled Release* **2012**, *161*, 592−599.
(9) Decher, G. *Science* **1997**, *277*, 1232−1237.
(10) Caruso, F.; Caruso, R. A.; Möhwald, H. *Science* **1998**, *282*, 1111−1114.
(11) Delcea, M.; Möhwald, H.; Stirtach, A.G. *Adv. Drug Delivery. Rev.* **2011**, *63*, 730−747.
(12) De Cock, L. J.; De Koker, S.; De Geest, B. G.; Grooten, J.; Vervaet, C.; Remon, J. P.; Sukhorukov, G. B.; Antipina, M. N. *Angew. Chem., Int. Ed.* **2010**, *49*, 6954−6973.
(13) Yan, Y.; Wang, Y.; Heath, J. K.; Nice, E. C.; Caruso, F. *Adv. Mater.* **2011**, *23*, 3916−3921.
(14) Sukhorukov, G. B.; Antipov, A. A.; Voigt, A.; Donath, E.; Möhwald, H. *Macromol. Rapid Commun.* **2001**, *22*, 44−46.
(15) Andreeva, D. V.; Gorin, D. A.; Sukhorukov, D. G. *Macromol. Rapid Commun.* **2006**, *27*, 931−936.
(16) Li, C.; Li, Z. Y.; Zhang, J.; Wang, K.; Gong, Y. H.; Luo, G. F.; Zhuo, R. X.; Zhang, X. Z. *J. Mater. Chem.* **2012**, *22*, 4623−4626.
(17) De Koker, S.; De Cock, L. J.; Rivera-Gil, P.; Parak, W. J.; Auzély Velty, R.; Vervaet, C.; Remon, J. P.; Grooten, J.; De Geest, B. G. *Adv. Drug Delivery Rev.* **2011**, *63*, 748−761.
(18) Tong, W. J.; Zhu, Y.; Wang, Z. P.; Gao, C. Y.; Möhwald, H. *Macromol. Rapid Commun.* **2010**, *31*, 1015−1019.
(19) Manna, U.; Patil, S. *J. Phys. Chem. B* **2008**, *112* (42), 13258−13263.
(20) Yan, Y.; Ochs, C. J.; Such, G. K.; Heath, J. K.; Nice, E. C.; Caruso, F. *Adv. Mater.* **2010**, *22*, 5298−5403.
(21) van de Manakker, F.; Vermonden, T.; van Nostrum, C. F.; Hennink, W. E. *Biomacromolecules* **2009**, *10*, 3157−3175.
(22) Wang, Z. P.; Feng, Z. Q.; Gao, C. Y. *Chem. Mater.* **2008**, *20*, 4194−4199.
(23) Xiao, W.; Chen, W. H.; Zhang, J.; Li, C.; Zhuo, R. X.; Zhang, X. Z. *J. Phys. Chem. B* **2011**, *115*, 13796−13802.
(24) Lee, E. S.; Gao, Z.; Bae, Y. H. *J. Controlled Release* **2008**, *132*, 164−170.
(25) Ulbrich, K.; Šubr, V. *Adv. Drug Delivery Rev.* **2004**, *56*, 1023−1050.
(26) Swain, S. M.; Whaley, F. S.; Ewer, M. S. *Cancer* **2003**, *97*, 2869−2878.
(27) Mitra, S.; Garu, U.; Ghosh, P. C.; Maitra, A. N. *J. Control. Release* **2011**, *74*, 317−323.
(28) Zhang, J.; Xu, X. D.; Liu, Y.; Liu, C. W.; Chen, X. H.; Li, C.; Zhuo, R. X.; Zhang, X. Z. *Adv. Funct. Mater.* **2012**, *22*, 1704−1710.
(29) Li, C.; Luo, G. F.; Wang, H. Y.; Zhang, J.; Gong, Y. H.; Cheng, S. X.; Zhuo, R. X.; Zhang, X. Z. *J. Phys. Chem. C* **2011**, *115*, 17651−17659.
(30) Quan, C. Y.; Chen, J. X.; Wang, H. Y.; Li, C.; Chang, C.; Zhang, X. Z.; Zhuo, R. X. *ACS Nano* **2010**, *4*, 4211−4219.
(31) Hassan, G. S.; El-Emam, A. A.; Gad, L. M.; Barghash, A. M. *Saudi Pharm. J.* **2010**, *18*, 123−128.
(32) Zhang, J.; Li, C.; Wang, Y.; Zhuo, R. X.; Zhang, X. Z. *Chem. Commun.* **2011**, *47*, 4457−4459.
(33) Sukhorukov, G. B.; Volodkin, D. V.; Günther, A. M.; Petrov, A. I.; Shenoy, D. B.; Möhwald, H. *J. Mater. Chem.* **2004**, *14*, 2073−2081.
(34) Ulbrich, K.; Subr, V. *Adv. Drug Delivery Rev.* **2004**, *56*, 1023−1050.
(35) Yuan, X. B.; Li, H.; Zhu, X. X.; Woo, H. G. *J. Chem. Technol. Biotechnol.* **2006**, *81*, 746−754.
(36) Gao, L.; Fei, J.; Zhao, J.; Cui, W.; Cui, Y.; Li, J. *Chem.—Eur. J.* **2012**, *18*, 3185−3192.
(37) Krämer, M.; Stumbé, J.F.; Türk, H.; Krause, S.; Komp, A.; Delineau, L.; Prokhorova, S.; Kautz, H.; Haag, R. *Angew. Chem., Int. Ed.* **2002**, *41*, 4252−4256.
(38) Vaupel, P.; Kallinowski, F.; Okunieff, P. *Cancer Res.* **1989**, *49*, 6449−6465.
(39) Hu, Q. D.; Fan, H.; Ping, Y.; Liang, W. Q.; Tang, G. P.; Li, J. *Chem. Commun.* **2011**, *47*, 5572−5574.
(40) Hu, Q. L.; Li, W.; Hu, X. R.; Hu, Q. D; Shen, J.; Jin, X.; Zhou, J.; Tang, G. P.; Chu, P. K. *Biomaterials* **2012**, *33*, 6580−6591.